

Cite this: *Dalton Trans.*, 2016, **45**,
3464Synthesis, structure and luminescent properties
of lanthanide fluoroalkoxides†D. M. Kuzyaev,^{*a} T. V. Balashova,^{a,b} M. E. Burin,^{a,b} G. K. Fukin,^{a,b} R. V. Rumyantsev,^a
A. P. Pushkarev,^a V. A. Ilichev,^{a,b} I. D. Grishin,^b D. L. Vorozhtsov^b and
M. N. Bochkarev^{*a,b}

Alkoxides [Ln(OR)₃(DME)]₂ (R = CH(CF₃)₂, Ln = Sm (**1**), Yb (**2**)), [Ce(OR)₃(Phen)]₂ (**3**) (Phen = 1,10-phenanthroline), [Ce(OR')₃(DME)]₂ (R' = C(CF₃)₃) (**4**), {Gd(OR')₃(DME)}₂ (**5**), {Ln₂[O(CF₃)₂C–C(CF₃)₂O]}₂ (Ln = Ce (**6**), Gd (**7**)), {Ce₂[O(CF₃)₂C–C(CF₃)₂O]}₂(Phen)₂ (**8**), and {Ce[O(CF₃)₂C–C(CF₃)₂O][O(CF₃)₂–C(CF₃)₂OH]}₂(Phen)₂ (**9**) were synthesized by the reactions of silylamides Ln[N(SiMe₃)₂]₃ with respective fluorinated alcohols. The heterovalent trinuclear complex {Sm₂(μ₂-OR)₃(μ₃-OR)₂Sm(OR)₂(THF)_{2.5}(Et₂O)_{0.5}} (**10**) was obtained by treatment of SmI₂(THF)₂ with ROK. The reaction of europium(II) and yttrium(III) silylamides with ROH afforded the heterobimetallic alkoxide {Eu₂(μ₂-OR)₃(μ₃-OR)Y(OR)₂(DME)}₂ (**11**) containing divalent europium. The molecular structures of **1**, **2**, **3**, **9**, **10** and **11** were determined by X-ray analysis. All the prepared cerium derivatives as well as the europium–yttrium isopropoxide upon UV excitation exhibited photoluminescence in the regions of 370–425 (for Ce³⁺) and 485 nm (for Eu²⁺) which was assigned to 4d→5f transitions.

Received 26th November 2015,
Accepted 5th January 2016

DOI: 10.1039/c5dt04636j

www.rsc.org/dalton

Introduction

Luminescent materials attract great attention because of their wide application in light sources and color displays, such as cell phones, computer and TV screens. In particular, organo-lanthanide emitters have inspired vigorous research activities owing to their long luminescence lifetimes and narrow characteristic emission bands originated from f–f transitions, which cover the entire visible and near-infrared region.¹ Besides, organic derivatives of cerium(III), gadolinium(III), europium(II), and ytterbium(II) can exhibit metal-centered emission in the UV-blue area and are attractive due to their potential application in the design of the excitation sources for chemical sensing devices, lithography, optical data recording and biomedicine.² The short-wave metal-centered luminescence of Ce³⁺, Eu²⁺ and Yb²⁺ occurs due to f–d transitions, which are parity-allowed, so the complexes of these metals have higher light outputs compared to f–f emitters.³ The luminescence of f–d transitions can be observed as well for the Sm²⁺ and Tm²⁺

ions but in this case, the emission wavelength is above 650 nm.⁴ Despite the attraction of these phosphors from the academic point of view and plausible application, the publications devoted to organo-lanthanide UV-blue emitters are scarce. Among the organocerium derivatives the UV luminescence was detected for the complexes of CeCl₃ with crown ethers⁵ and bipyridine,⁶ and for the pyrazinecarboxylate⁷ and alkylamine trifluoromethanesulfonate.⁸ The only known organogadolinium UV emitter is the diethylenetriaminepentaacetate, which revealed f–f photoluminescence (PL) at 312 nm.⁹ Short-wavelength emission of Eu²⁺ was found for the europium(II) chlorides and bromides with crown-ether, azacrown-ether and cryptand ligands.¹⁰ The sole organoderivative of divalent lanthanide for which the electroluminescence (EL) was documented is europium(II) bis[tris(dimethylpyrazolyl)borate].¹¹ The EL spectrum of this complex contains a weak band at 430 nm, which was assigned to f–d transition.

Recently we have reported the preparation, structures and luminescent properties of fluorinated isopropoxides of Ce(III), Eu(II/III), Gd(III), Tm(III) and Yb(II/III).¹² The PL (λ_{em} = 330 nm) was found only for europium complex Eu₃(OR^F)₇(DME)₂. In continuation of these studies and in search of new UV-blue phosphors, we have synthesized a set of new fluorinated isopropoxides, *tert*-butoxides and 2,3-butanediolates of Ce(III), Sm(II/III), Eu(II), Gd(III) and Yb(III). Fluorinated alkoxide ligands were chosen because: (i) eliminating of C–H groups (which are well known luminescence quenchers) facilitates emitting efficiency;¹³ (ii) fluorine substituents improve the hydrolytic

^aG. A. Razuvaev Institute of Organometallic Chemistry, Russian Academy of Sciences, Tropinina Street 49, 603137 Nizhny Novgorod, Russia. E-mail: mboch@iomc.ras.ru, kuzyaev@iomc.ras.ru

^bNizhny Novgorod State University, Gagarina Avenue 23/2, 603950 Nizhny Novgorod, Russia

† Electronic supplementary information (ESI) available: Details of X-ray experiments, crystallographic, collection and refinement data for the complexes 1–3, 9–11. CCDC 1437390–1437395. For ESI and crystallographic data in CIF or other electronic format see DOI: 10.1039/c5dt04636j



and thermal stability, and enhance the volatility of the compounds¹⁴ which are important in the preparation of OLED devices by the vacuum deposition method; (iii) the polyfluorinated ligands can provide high-energy metal–ligand charge transfer state (MLCT) and short-wavelength emission.¹²

Experimental section

All experiments were performed in evacuated tubes using standard Schlenk techniques, thus excluding traces of air and water. The solvents were purified by distillation from sodium/benzophenone ketyl (THF, DME, diethyl ether) and sodium (hexane, toluene). MeCN for electron spectroscopy, ROH, R'OH, HO(CF₃)₂C–C(CF₃)₂OH, 1,10-phenanthroline, and Ln[N(SiMe₃)₂]₃ (Ln = Ce, Gd, Sm, Yb, Dy, Y), were purchased from commercial suppliers. Iodide SmI₂(THF)₂ and silylamide complex Eu[N(SiMe₃)₂]₂(DME)₂ were prepared according to the published procedures.^{15,16} IR spectra were recorded on a Specord M-75 instrument in the region of 4000–450 cm⁻¹. The C, H, N elemental analyses were performed by using the Vario El cube CHNS elemental analyzer (Nizhny Novgorod State University). Yttrium and lanthanide contents were analysed by complexometric titration. Magnetic susceptibility measurements were carried out according to the procedure.¹⁷ Absorption spectra were recorded on a UV/VIS instrument “Perkin-Elmer Lambda-25” from 200 to 800 nm. Emission spectra were registered from 220 to 700 nm on a fluorescent spectrometer “Perkin Elmer LS-55”. Registration of absorption and emission spectra were performed in a 1 cm fluorescent quartz cuvette.

[Sm(OR)₃(DME)]₂ (1)

Propanol ROH (0.094 g, 0.56 mmol) was condensed to the solution of Sm[N(SiMe₃)₂]₃ (0.123 g, 0.19 mmol) in 10 ml of DME. The reaction mixture was stirred for 3 h. The solvent was removed by condensation *in vacuo* and the residue was recrystallized from the mixture PhCH₃–Et₂O. Yield of the product is 0.108 g (77%). Anal. calcd (%) for C₂₆H₂₆F₃₆O₁₀Sm₂ (1483.14): C, 21.06; H, 1.77; Sm, 20.28. Found (%): C, 20.89; H, 1.74; Sm, 20.59. IR (ν, cm⁻¹): 3654 (w), 3380 (w), 1626 (w), 1285 (m), 1258 (w), 1216 (m), 1182 (m), 1094 (m), 890 (w), 848 (w), 742 (w), 722 (w), 687 (w).

[Yb(OR)₃(DME)]₂ (2)

Complex 2 was prepared similarly to 1 from Yb[N(SiMe₃)₂]₃ (0.272 g, 0.42 mmol) and ROH (0.215 g, 1.28 mmol). Yield of the product is 0.213 g (66%). Mp: 158–160 °C. Anal. calcd (%) for C₂₆H₂₆F₃₆O₁₀Yb₂ (1528.50): C, 20.43; H, 1.71; Yb, 22.64. Found (%): C, 20.71; H, 1.95; Yb, 22.76. The IR spectrum of the product is analogous to that of complex 1.

[Ce(OR)₃(Phen)]₂ (3)

A solution of ROH (0.209 g, 1.24 mmol) and 1,10-phenanthroline (0.071 g, 0.39 mmol) in 10 ml of PhCH₃ was added to a solution of Ce[N(SiMe₃)₂]₃ (0.238 g, 0.38 mmol) in 10 ml of PhCH₃. The reaction mixture was stirred at 70 °C for 4 h. The

precipitated yellow crystals were filtered off and washed with cold PhCH₃ (2 × 10 ml). Drying of the crystals gave 0.219 g (70%) of complex 3. Mp: 147–148 °C (dec.). Anal. calcd (%) for C₄₂H₂₂Ce₂F₃₆N₄O₆ (1642.82): C, 31.70; H, 1.33; Ce, 16.81; N, 3.36. Found (%): C, 31.82; H, 1.35; Ce, 16.84; N, 3.47. IR (ν, cm⁻¹): 3658 (w), 3456 (w), 1628 (w), 1593 (w), 1580 (w), 1521 (m), 1499 (w), 1428 (w), 1286 (s), 1260 (m), 1213 (s), 1183 (s), 1126 (w), 1095 (s), 887 (m), 864 (w), 855 (m), 845 (s), 771 (w), 741 (m), 731 (m), 687 (s), 644 (w), 521 (w).

[Ce(OR')₃(DME)₂]₂ (4)

Complex 4 was prepared similarly to 1 from butanol R'OH (0.266 g, 1.13 mmol) and Ce[N(SiMe₃)₂]₃ (0.167 g, 0.27 mmol). Yield of the product is 0.197 g (72%). Mp: 171 °C (dec.). Anal. calcd (%) for C₄₀H₄₀Ce₂F₃₄O₁₄ (2050.88): C, 23.43; H, 1.97; Ce, 13.66. Found (%): C, 23.24; H, 1.78; Ce, 13.42. IR (ν, cm⁻¹): 3691 (w), 3606 (w), 3403 (w), 1231 (s, br), 1097 (m), 1050 (s), 1017 (w), 966 (s), 858 (s), 768 (m), 726 (s), 708 (m), 569 (w), 536 (m).

{Gd(OR')₃(DME)₂} (5)

Complex 5 was prepared similarly to 1 from butanol R'OH (0.173 g, 0.73 mmol) and Gd[N(SiMe₃)₂]₃ (0.149 g, 0.23 mmol). Yield of the complex 5 is 0.162 g (67%). Mp: 152 °C (dec.). Anal. calcd (%) for C₂₀H₂₀GdF₂₇O₇ (1042.58): C, 23.04; H, 1.93; Gd, 15.08. Found (%): C, 22.91; H, 2.05; Gd, 15.43. The IR spectrum of the product is analogous to that of 4.

{Ce₂[O(CF₃)₂C–C(CF₃)₂O]₃} (6)

Butanediol HO(CF₃)₂C–C(CF₃)₂OH (0.120 g, 0.36 mmol) was added by condensation *in vacuo* to a solution of Ce[N(SiMe₃)₂]₃ (0.140 g, 0.23 mmol) in 10 ml THF. The reaction mixture was stirred for 3 h. The solvent was removed by condensation *in vacuo*. Recrystallization of the residue from the mixture THF–Et₂O gave colorless crystals of complex 6 (0.109 g, 76%). Mp: 110–112 °C (dec.). Anal. calcd (%) for C₁₈Ce₂F₃₆O₆ (1276.36): C, 16.94; Ce, 21.96. Found (%): C, 16.79; Ce, 21.68. IR (ν, cm⁻¹): 3684 (w), 1238 (s, br), 1052 (w), 936 (m), 872 (m), 759 (w), 739 (m), 720 (m), 704 (w), 674 (w), 542 (w).

{Gd₂[O(CF₃)₂C–C(CF₃)₂O]₃} (7)

Complex 7 was prepared similarly to 1 from butanediol HO(CF₃)₂C–C(CF₃)₂OH (0.130 g, 0.39 mmol) and Gd[N(SiMe₃)₂]₃ (0.156 g, 0.24 mmol). Yield of the product is 0.137 g (86%). Mp: 142 °C (dec.). Anal. calcd (%) for C₁₈F₃₆Gd₂O₆ (1310.63): C, 16.50; Gd, 24.00. Found (%): C, 16.71; Gd, 23.76. The IR spectrum of the product is analogous to that of 6.

{Ce₂[O(CF₃)₂C–C(CF₃)₂O]₃(Phen)₂} (8)

A solution of Ce[N(SiMe₃)₂]₃ (0.243 g, 0.39 mmol) and 1,10-phenanthroline (0.075 g, 0.42 mmol) in 10 ml of THF was added to a solution of HO(CF₃)₂C–C(CF₃)₂OH (0.207 g, 0.62 mmol) in 5 ml of THF. The reaction mixture was stirred for 3 h. The solvent was removed by condensation *in vacuo*. The resulting pale-brown solid was washed with hexane (3 × 15 ml) and dried. Recrystallization of the residue from the mixture DME–PhCH₃ gave orange crystals of complex 9



(0.022 g, 5%) which were isolated *via* decantation of the supernatant solution. After evaporation of the solvent from the mother liquor *in vacuo* and washing of the residue with hexane (2 × 10 ml), alkoxide **8** was obtained as a pale-brown solid. Yield of the product was 0.266 g (83%). Mp: 135 °C (dec.). Anal. Calcd (%) for C₄₂H₁₆Ce₂F₃₆N₄O₆ (1636.77): C, 30.82; H, 0.99; N, 3.42. Found (%): C, 30.94; H, 1.06; N, 3.39. IR (ν , cm⁻¹): 3670 (w), 1674 (w), 1629 (w), 1592 (w), 1577 (w), 1520 (m), 1500 (w), 1427 (m), 1349 (w), 1235 (s, br), 1059 (w), 987 (w), 969 (w), 930 (s), 891 (w), 866 (s), 846 (m), 758 (w), 739 (m), 733 (s), 716 (s), 704 (w), 669 (w), 638 (w), 541 (w).

{Ce[O(CF₃)₂C-C(CF₃)₂O][O(CF₃)₂C-C(CF₃)₂(OH)](Phen)₂} (**9**)

A solution of Ce[N(SiMe₃)₂]₃ (0.100 g, 0.16 mmol) and 1,10-phenanthroline (0.058 g, 0.32 mmol) in 10 ml of THF was added to a solution of HO(CF₃)₂C-C(CF₃)₂OH (0.108 g, 0.32 mmol) in 5 ml of THF. The reaction mixture was stirred for 3 h. The solvent was removed by condensation *in vacuo*. The resulting pale-brown solid was washed with hexane (3 × 15 ml) and dried. Recrystallization of the product from the mixture DME-PhCH₃ gave complex **9** as orange crystals (0.110 g, 59%). Mp: 180–185 °C (dec.). Anal. Calcd (%) for C₃₆H₁₇CeF₂₄N₄O₄ (1165.62): C, 37.09; H, 1.47; N, 4.81. Found (%): C, 37.27; H, 1.53; N, 4.65. IR (ν , cm⁻¹): 3085 (w), 1627 (w), 1592 (w), 1577 (w), 1518 (s), 1497 (w), 1426 (s), 1228 (s, br), 986 (m), 960 (w), 927 (s), 866 (s), 848 (s), 773 (w), 731 (s), 713 (m), 686 (w), 637 (w), 528 (w, br), 467 (w).

{Sm₂(μ_2 -OR)₃(μ_3 -OR)₂Sm(OR)₂(THF)_{2.5}(Et₂O)_{0.5}} (**10**)

A solution of SmI₂(THF)₂ (0.351 g, 0.64 mmol) in 10 ml of THF was added to a solution of ROK (prepared from 0.050 g (1.25 mmol) of KH and 0.236 g (1.40 mmol) of ROH according to the known procedure) in 10 ml of THF. The reaction mixture was stirred for 5 h. The precipitate of KI was filtered off and the solvent from the resulting solution was removed by condensation *in vacuo*. The residue was extracted with diethyl ether (4 × 10 ml). After concentrating and cooling of the extract, dark red crystals of **10** (0.155 g, 40%) were obtained. $\mu_{\text{eff}} = 2.91\mu_{\text{B}}$. Anal. calcd (%) for C₃₃H₃₂F₄₂O₁₀Sm₃ (1837.61): C, 21.57; H, 1.76; Sm, 24.55. Found (%): C, 21.29; H, 1.70; Sm, 24.84. The IR spectrum of the product is similar to that of complex **1**.

{Eu₂(μ_2 -OR)₃(μ_3 -OR)₂Y(OR)₂(DME)₂} (**11**)

A solution of ROH (0.158 g, 0.94 mmol) in 5 ml of Et₂O was added slowly to a solution of Y[N(SiMe₃)₂]₃ (0.072 g, 0.13 mmol) and Eu[N(SiMe₃)₂]₂(DME)₂ (0.157 g, 0.24 mmol) in 10 ml of Et₂O. The reaction mixture was stirred for 3 h. The product was obtained as pale greenish-yellow crystals after concentrating and cooling of the resulting solution (0.115 g, 55%). Mp: 208–210 °C (dec.). Anal. calcd (%) for C₂₉H₂₇Eu₂F₄₂O₁₁Y (1742.28): C, 19.99; H, 1.56. Found (%): C, 20.28; H, 1.80. The IR spectrum of the product is similar to that of the complex **1**.

Device fabrication

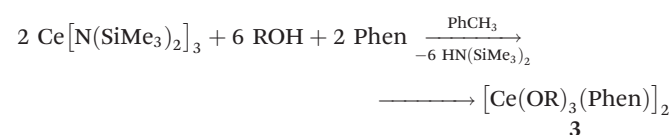
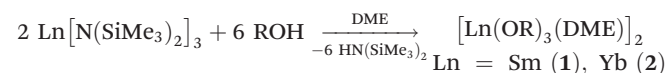
The three-layer device of structure ITO/TPD (30 nm)/complex **3** (50 nm)/BATH (20 nm)/Yb, consisting of triphenyldiamine derivative (TPD) as a hole transport layer, 4,7-diphenyl-1,10-phenanthroline (BATH) as an electron-transporting and hole-blocking layer and the lanthanide complex as an emission layer, was fabricated in a vacuum chamber (10⁻⁶ mbar) with different resistive heaters for organic and metal layers. A commercial ITO on a glass substrate with 5 Ω sq.⁻¹ was used as the anode material (Luminescence Technology Corp.) and commercial Yb, 99.9% trace metal basis (Sigma-Aldrich) as the cathode material. The deposition rate for the organic compounds and metal complex was 1 nm s⁻¹. The active area of the device was 5 × 5 mm. The EL spectra and current-voltage characteristics were measured using an Ocean Optics USB-2000 fluorimeter, the computer controlled GW Instek PPE 3323 power supply and a GW Instek GDM 8246 digital multimeter under ambient conditions.

Results and discussion

Synthesis

Isopropoxides **1** and **2** were prepared by reactions of respective silylamides Ln[N(SiMe₃)₂]₃ (Ln = Sm, Yb) and hexafluoroisopropanol in DME solution. To synthesize cerium isopropoxide **3** in the reaction mixture phenanthroline was added. Note that complexes **1** and **2** have been prepared earlier,¹⁸ but their structures and luminescent properties have not been studied.

The products were isolated from the ether-toluene mixture as microcrystalline powders soluble in THF, diethyl ether, and DME. Unlike hydrolyzed and nonsublimable **1** and **2**, cerium isopropoxide **3**, due to the presence of the shielding phenanthroline at the metal center, is relatively stable in air and can be sublimed *in vacuo* without decomposition which made it possible to design the OLED device on its base and study the EL properties (*vide infra*).



X-ray analysis revealed that complexes **1** and **2** are centrosymmetrical, and isostructural dimeric compounds (Fig. 1) and have the arrangement quite analogous to that of the Ce and Tm isopropoxides reported earlier.¹² In alkoxides **1** and **2** two lanthanide ions are linked *via* two bridging μ_2 -OR groups, each ion is bonded with two terminal isopropoxide groups and one DME molecule. The terminal Ln–O distances (2.130(5)–2.182(4) in **1** and 2.068(3)–2.092(3) Å in **2**) are notably shorter compared to the bridging ones (2.368(4)–2.408(3) in **1** and 2.279(3)–2.284(3) in **2**). The Yb...Yb distance in **2** is equal to



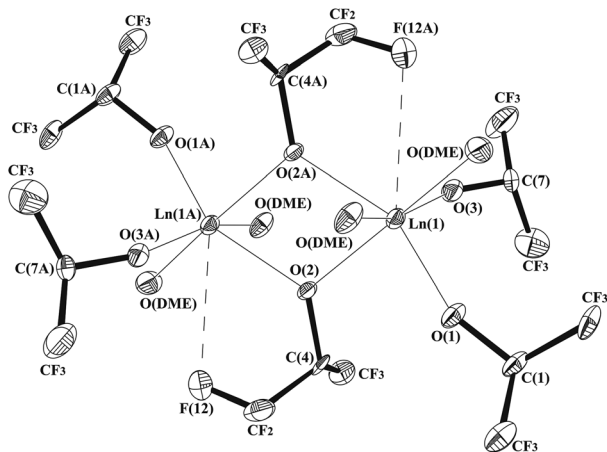


Fig. 1 Molecular structures of **1** (Ln = Sm) and **2** (Ln = Yb). Thermal ellipsoids are drawn at the 30% probability level. H atoms are omitted for clarity. Selected distances [Å] and angles [°] in **1**: Sm(1)–O(3) 2.130(5), Sm(1)–O(1) 2.182(4), Sm(1)–O(2) 2.368(4), Sm(1)–O(2A) 2.408(3), Sm(1)–O(5) 2.459(4), Sm(1)–O(4) 2.514(4), Sm(1)–F(12A) 2.852(4), Sm(1)–Sm(1A) 3.9452(9); O(3)–Sm(1)–O(1) 101.43(16), O(3)–Sm(1)–O(2) 106.75(17), O(1)–Sm(1)–O(2) 85.29(14), O(3)–Sm(1)–O(2A) 100.55(15), O(1)–Sm(1)–O(2A) 149.75(15), O(2)–Sm(1)–O(2A) 68.59(15), O(3)–Sm(1)–F(12A) 75.66(15), O(1)–Sm(1)–F(12A) 146.17(13), O(2)–Sm(1)–F(12A) 128.20(11), O(2A)–Sm(1)–F(12A) 60.40(12); in **2**: Yb(1)–O(3) 2.068(3), Yb(1)–O(1) 2.092(3), Yb(1)–O(2) 2.279(3), Yb(1)–O(2A) 2.284(3), Yb(1)–O(4) 2.356(4), Yb(1)–O(5) 2.388(4), Yb(1)–F(12A) 3.056(4), Yb(1)–Yb(1A) 3.7294(4); O(3)–Yb(1)–O(1) 100.84(13), O(3)–Yb(1)–O(2) 105.48(13), O(1)–Yb(1)–O(2) 87.84(13), O(3)–Yb(1)–O(2A) 99.36(12), O(1)–Yb(1)–O(2A) 153.56(13), O(2)–Yb(1)–O(2A) 70.38(12), O(2A)–Yb(1)–F(12A) 69.49(11), O(1)–Yb(1)–F(12A) 145.07(13), O(2)–Yb(1)–F(12A) 126.93(11), O(2A)–Yb(1)–F(12A) 59.30(10). Symmetry transformations were used to generate equivalent atoms: $-x + 1, -y + 1, -z + 1$ in **1** and **2**.

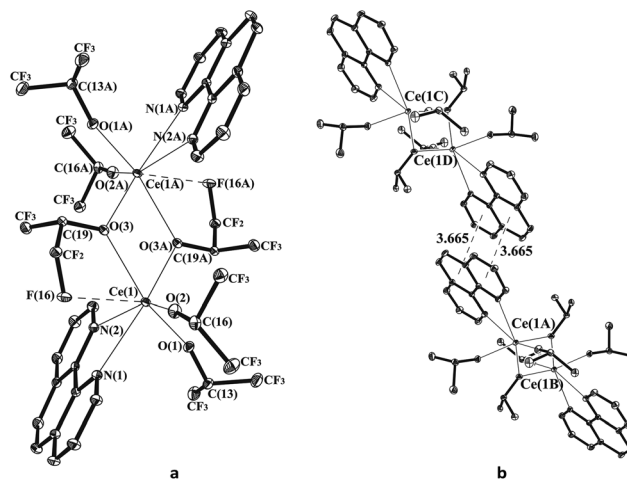


Fig. 2 Molecular structure of **3** (a) and the dimeric structure of **3** in crystal (b). Thermal ellipsoids are drawn at the 30% probability level. H atoms are omitted for clarity. Selected distances [Å] and angles [°] in **3**: Ce(1)–O(2) 2.2064(15), Ce(1)–O(1) 2.2340(15), Ce(1)–O(3A), 2.4394(15) Ce(1)–O(3) 2.5249(15), Ce(1)–N(1) 2.6488(18), Ce(1)–N(2) 2.6567(17), Ce(1)–F(16) 2.9182(14), Ce(1)–Ce(1A) 4.1305(2); O(2)–Ce(1)–O(1) 99.46(6), O(2)–Ce(1)–O(3A) 113.65(6), O(1)–Ce(1)–O(3A) 88.35(6), O(2)–Ce(1)–O(3) 99.96(6), O(1)–Ce(1)–O(3) 153.53(6), O(3A)–Ce(1)–O(3) 67.40(6), O(2)–Ce(1)–N(1) 87.50(6), O(1)–Ce(1)–N(1) 84.37(6), O(3A)–Ce(1)–N(1) 158.54(5), O(2)–Ce(1)–F(16) 76.00(5), O(1)–Ce(1)–F(16) 144.16(5), O(3A)–Ce(1)–F(16) 126.44(4), O(3)–Ce(1)–F(16) 59.06(4).

3.7294(4) that is shorter than the Sm...Sm one in **1** (3.9452 Å). It is interesting to note that there are close intramolecular contacts Sm(1)...F(12A) (Sm(1A)...F(12)) in **1** whereas the analogous interactions in **2** are absent. Really, the Yb(1)...F(12A) distance in **2** is 3.056(4) Å and notably exceeds the analogous one in **1** (2.852(4) Å). According to the literature data,^{19–22} typical interval values for intramolecular Yb...F and Sm...F interactions are 2.48(1)–2.726(9) Å and 2.537(2)–2.813(3) Å respectively. Besides, the intramolecular Sm(1A)...F(12) interaction leads to elongation of the C(6A)–F(12A) (1.364(7) Å) bond length compared to other distances in this CF₃ group (1.317(8)–1.329(8) Å). In order to understand why the intramolecular Yb(1A)...F(12) interactions are absent in **2**, we have analyzed the saturation of the metal coordination sphere (G-parameter)²³ in these complexes. According to our calculations the saturation of the metal coordination sphere by ligands in **2** is 97.3 (2)% that markedly exceeds the analogous one in **1** (94.9 (2)%). Thus, there is insufficient room around the metal in **2** to realize an additional Yb...F interaction. In other words, steric factors inhibit realization of the intramolecular Yb...F contact in **2**.

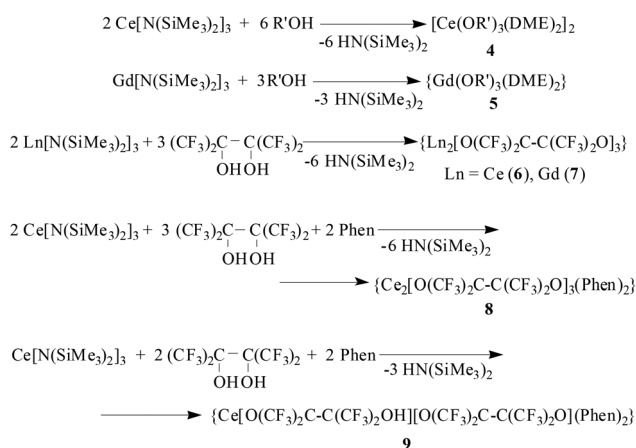
According to X-ray data complex **3** has a centrosymmetrical, dimeric structure (Fig. 2a) which is close to that of **1** and **2**.

The main difference of complex **3** from **1** and **2** lies in coordination phenanthroline molecules instead of the DME ones. Cerium ions are linked by two μ_2 -bridged OR ligands. Each metal ion is bound to two terminal isopropoxide groups and one phenanthroline molecule. The distance Ce...Ce(1A) (4.1305(2) Å) is slightly longer than that in the complex Ce₂(OR)₆(DME)₂ (4.064 Å).¹² As in **1** the intramolecular Ce...F interactions in **3** are realized. The Ce(1)...F(16) distance (2.9182(14) Å) exceeds the analogous distances in **1** and lies within the interval of values for published data (2.6248(16)–2.9206(13) Å).^{24,25} As one should expect that such an interaction leads to elongation of the C(21)–F(16) bond length (1.362(2) Å) compared to other distances in this CF₃-group (1.330(3)–1.339(3) Å). The steric saturation of the metal coordination sphere by ligands in **3** is 90.5 (2)% that is less than in **2**. Thus, the steric factors do not prevent the realization of the intramolecular Ce...F interaction in **3** as it is distinct from **1**. Due to the presence of phenanthroline containing extensive π -systems, in a crystal of **3**, intermolecular π ... π interactions are realized which combine the molecules in couples (Fig. 2b). The distances between centers of six-membered rings are 3.665 Å and satisfy the geometric criterion for the existence of π ... π interactions (3.8 Å)²⁶ between phenanthroline molecules in neighboring complexes.

Perfluorinated *tert*-butoxides **4**, **5** and diolates **6**, **7**, **8** were prepared similarly to **1**–**3**. In the reactions with the diol, the molar ratio 2 : 3 was used. The butoxides contain two molecules of DME whereas diolates have no coordinated solvent at all. LDI-TOF analysis revealed that cerium *tert*-butoxide is a



dimer while the gadolinium counterpart has a monomeric structure.



Besides the pale brown product **8** in the last reaction, a negligible amount of mononuclear diolate $\{\text{Ce}[\text{O}(\text{CF}_3)_2\text{C}-\text{C}(\text{CF}_3)_2\text{O}][\text{O}(\text{CF}_3)_2\text{C}-\text{C}(\text{CF}_3)_2(\text{OH})](\text{Phen})_2\}$ (**9**) was isolated as orange crystals. Change of the cerium amide:diol ratio to 1:2 resulted in an increase of the yield of **9** up to 59%. Probably, the reason for formation of such a product is due to a slight excess of alcohol and phenanthroline in the reaction mixture.

According to X-ray analysis complex **9** (Fig. 3a) has a monomeric structure in which the cerium ion is linked to one butanediolate, one hydroxybutanediolate and two phenanthroline ligands. The cerium–oxygen distances of the butanediolate ligand (2.311(4) and 2.344(4) Å) are significantly longer than the length of the cerium–oxygen bond of the hydroxybutane-

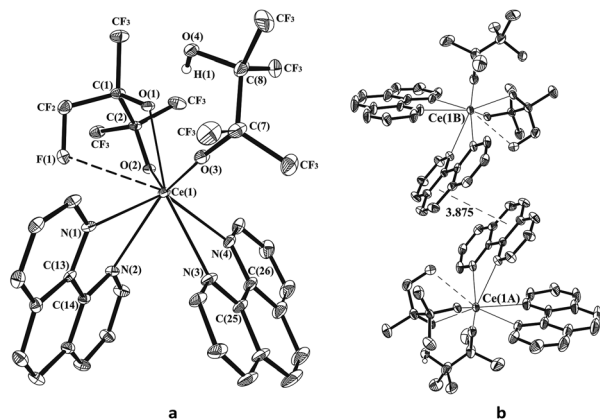


Fig. 3 Molecular structure of **9** (a) and the dimeric structure of **9** in crystal (b). Thermal ellipsoids are drawn at the 30% probability level. H atoms are omitted for clarity. Selected distances [Å] and angles [°] in **9**: Ce(1)–O(3) 2.258(5), Ce(1)–O(2) 2.311(4), Ce(1)–O(1) 2.344(4), Ce(1)–N(2) 2.648(5), Ce(1)–N(1) 2.653(6), Ce(1)–N(4) 2.679(6), Ce(1)–N(3) 2.741(6), Ce(1)–F(1) 2.950(4); O(3)–Ce(1)–O(2) 136.86(17), O(3)–Ce(1)–O(1) 75.95(16), O(2)–Ce(1)–O(1) 66.80(15), O(3)–Ce(1)–N(2) 139.64(18), O(2)–Ce(1)–N(2) 83.17(16), O(1)–Ce(1)–N(2) 131.94(16), O(3)–Ce(1)–F(1) 115.54(16), O(2)–Ce(1)–F(1) 62.61(15), O(1)–Ce(1)–F(1) 59.63(14), N(1)–Ce(1)–F(1) 64.77(15), N(3)–Ce(1)–F(1) 137.70(17).

diolate group (2.258(5) Å). Such differences in the bond lengths can be caused by steric effects in the coordination sphere of cerium. In complex **9** as for **3** there is an intramolecular Ce(1)⋯F(1) (2.950(4) Å) interaction which leads to the elongation of the bond C(3)–F(1) (1.353(9) Å) length compared to analogous ones (1.337(9)–1.341(9) Å). The steric saturation of the metal coordination sphere by ligands in **3** is 87.7(2)%. It should be noted that phenanthroline molecules neighboring complexes **9** in the crystal have offset disposition to each other but the distance between the centers of the six-membered rings of these ligands (3.875 Å) slightly exceeds the geometric criterion for the existence of the π – π interaction (Fig. 3b).²⁶

The general properties of alkoxides **4**–**9** are similar to those of isopropoxides **1** and **3**: they are slowly hydrolyzed in air, soluble in common organic solvents and do not sublime *in vacuo* which prevents their application as an emitting material in OLED devices.

As it has been mentioned, f–d emission of lanthanide complexes is of considerable interest because of their wide application potential. In an effort to obtain samarium(II) the f–d emitter, interaction of SmI_2 with potassium isopropoxide KOR was carried out. However, the reaction afforded the complex $\{\text{Sm}_2(\mu_2\text{-OR})_3(\mu_3\text{-OR})_2\text{Sm}(\text{OR})_2(\text{THF})_{2.5}(\text{Et}_2\text{O})_{0.5}\}$ (Fig. 4) containing one Sm^{3+} and two Sm^{2+} cations.

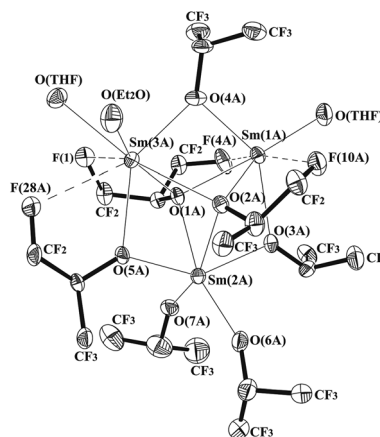
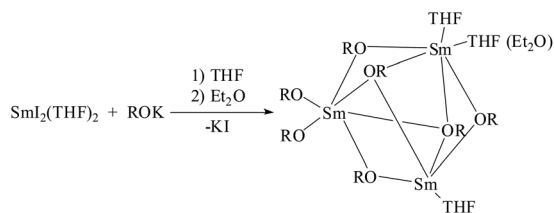


Fig. 4 Molecular structure of **10**. Thermal ellipsoids are drawn at the 30% probability level. H atoms are omitted for clarity. Selected distances [Å] and angles [°] in **10**: Sm(1A)–O(3A) 2.486(11), Sm(1A)–O(1A) 2.555(10), Sm(1A)–O(2A) 2.605(11), Sm(1A)–F(10A) 2.720(11), Sm(1A)–F(4A) 2.728(10), Sm(1A)–Sm(2A) 3.7253(12), Sm(1A)–Sm(3A) 3.8026(12), Sm(2A)–O(7A) 2.155(11), Sm(2A)–O(6A) 2.201(11), Sm(2A)–O(3A) 2.350(10), Sm(2A)–O(5A) 2.364(10), Sm(2A)–O(2A) 2.477(11), Sm(2A)–O(1A) 2.512(10), Sm(2A)–Sm(3A) 3.7568(11), Sm(3A)–O(4A) 2.410(12), Sm(3A)–O(5A) 2.519(10), Sm(3A)–O(2SA) 2.590(11), 2.596(5), Sm(3A)–O(2A) 2.617(11), Sm(3A)–O(1A) 2.663(10), Sm(3A)–F(28A) 2.894(11); O(3A)–Sm(1A)–O(1A) 71.8(3), O(3A)–Sm(1A)–O(4A) 136.0(3), O(1A)–Sm(1A)–O(4A) 76.0(4), O(3A)–Sm(1A)–O(2A) 69.0(3), O(1A)–Sm(1A)–O(2A) 64.5(3), O(4A)–Sm(1A)–O(2A) 70.5(4), O(3A)–Sm(1A)–F(10A) 85.0(4), O(1A)–Sm(1A)–F(10A) 125.6(3), O(4A)–Sm(1A)–F(10A) 90.2(4), O(2A)–Sm(1A)–F(10A) 61.3(3), O(1A)–Sm(1A)–F(4A) 60.5(3), O(4A)–Sm(1A)–F(4A) 104.8(4), O(2A)–Sm(1A)–F(4A) 124.0(3), Sm(2A)–Sm(1A)–Sm(3A) 59.86(2).

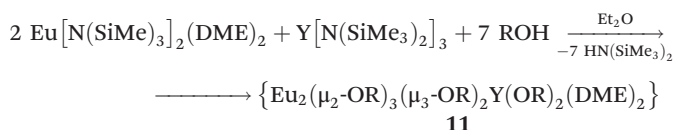




Formation of heterovalent product can be stipulated by the reaction of the formed at initial stage samarium(II) isopropoxide with ROH which remains after the synthesis of potassium salt and its excess cannot be removed from the reaction solution without decomposition of this salt.

According to the X-ray analysis, the metal atoms in **10** are linked to each other *via* μ_2 - and μ_3 -isopropoxide ligands. Two terminal OR groups are bonded to the Sm^{3+} ion. The μ_3 -oxygen atoms (O(1) and O(2)) are disposed over and under the plain $\text{Sm}(1)\text{Sm}(2)\text{Sm}(3)$ forming the trigonal-bipyramidal skeleton. Note that there are two independent molecules of **10** in the asymmetric unit cell. The Sm^{2+} cations in one of the independent molecules of **10** are coordinated by three THF molecules whereas in other molecules they are coordinated by one Et_2O and two THF molecules. Additionally, there are four close contacts between samarium(II) ions and fluorine atoms of μ_3 -OR ligands in the complex.

Another potential f-d emitter – heterobimetallic alkoxide of divalent europium $\{\text{Eu}_2(\mu_2\text{-OR})_3(\mu_3\text{-OR})_2\text{Y}(\text{OR})_2(\text{DME})_2\}$ (**11**) was synthesized by the reaction of $\text{Y}[\text{N}(\text{SiMe}_3)_2]_3$ and $\text{Eu}[\text{N}(\text{SiMe}_3)_2]_2$ with isopropanol in Et_2O solution. Yttrium was chosen as a sensitizer of europium emission because it can form high-lying ligand-to-metal charge transfer state (LMCT) from which transfer of absorbing energy to resonance levels of Eu(II) may occur.¹² It should be noted that compound **11** is the first structurally characterized heterobimetallic complex, which contains yttrium and europium ions (Fig. 5).



In spite of the fact that complexes **10** and **11** were prepared by different reactions, the molecular structures of these compounds are very similar. Moreover, arrangement of the prepared earlier complexes $\text{Eu}_3(\text{OR})_7(\text{DME})_2$ and $\text{Yb}_3(\text{OR})_7(\text{THF})(\text{Et}_2\text{O})$ ¹² appeared to be analogous to that of complexes **10** and **11**. In both complexes one trivalent and two divalent metal cations are linked to each other *via* three μ_2 - and two μ_3 -isopropoxide ligands. Two terminal OR groups are bonded to Sm^{3+} (in **10**) and Y^{3+} (in **11**) ions. Two coordination sites around each of divalent ions are occupied by Et_2O and THF molecules in samarium isopropoxide and by DME in europium–yttrium complex. The μ_3 -oxygen atoms (O(1), O(2) in **10** and O(10), O(11) in **11**) are disposed over and under the plain $\text{Sm}(1)\text{Sm}(2)\text{Sm}(3)$ ($\text{Y}(1)\text{Eu}(1)\text{Eu}(2)$) forming the trigonal-bipyramidal skeleton. Six-membered metallacycle Ln_3O_3 in **10** and **11** is essentially flat. The largest deviation from the plane of atom metallacycle is 0.112 Å in **10** and 0.191 Å in **11**.

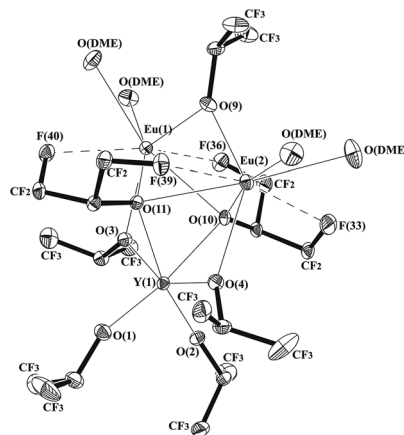


Fig. 5 Molecular structure of **11**. Thermal ellipsoids are drawn at the 30% probability level. H atoms are omitted for clarity. Selected distances [Å] and angles [°] in **10**: Y(1)–O(2) 2.115(3), Y(1)–O(1) 2.117(3), Y(1)–O(3) 2.277(3), Y(1)–O(4) 2.283(3), Y(1)–O(11) 2.365(3), Y(1)–O(10) 2.370(3), Y(1)–Eu(1) 3.6644(4), Y(1)–Eu(2) 3.6733(4), Eu(1)–O(9) 2.475(3), Eu(1)–O(11) 2.525(3), Eu(1)–O(3) 2.546(3), Eu(1)–F(36) 2.662(2), Eu(1)–O(10) 2.760(3), Eu(1)–F(40) 2.857(2), Eu(1)–Eu(2) 3.8602(3), Eu(2)–O(9) 2.473(3), Eu(2)–O(4) 2.530(3), Eu(2)–O(10) 2.536(3), Eu(2)–F(39) 2.678(2), Eu(2)–O(11) 2.811(3), Eu(2)–F(33) 2.974(3); O(2)–Y(1)–O(1) 99.51(11), O(2)–Y(1)–O(3) 95.43(11), O(1)–Y(1)–O(3) 106.76(11), O(3)–Y(1)–O(4) 148.63(10), O(2)–Y(1)–O(11) 165.27(10), O(1)–Y(1)–O(11) 94.95(10), O(3)–Y(1)–O(11) 77.57(9), O(4)–Y(1)–O(11) 76.07(9), O(2)–Y(1)–O(10) 94.32(10), O(1)–Y(1)–O(10) 165.17(10), O(11)–Y(1)–O(10) 71.59(9), O(9)–Eu(1)–O(11) 75.60(9), O(9)–Eu(1)–O(3) 134.29(9), O(11)–Eu(1)–O(3) 70.00(8), O(9)–Eu(1)–F(36) 89.58(9), O(3)–Eu(1)–F(36) 84.05(8), O(11)–Eu(1)–O(10) 63.01(8), F(36)–Eu(1)–F(40) 165.34(8).

The $\text{Sm}^{3+}\text{-}\mu_2\text{-O}$ distances (2.340(11)–2.364(10) Å) in **10** are somewhat shorter than the lengths of analogous $\text{Sm}^{2+}\text{-}\mu_2\text{-O}$ (2.410(12)–2.571(13) Å) due to a smaller radius of the Sm^{3+} ion compared to the Sm^{2+} one (1.098(CN = 6), 1.360(CN = 7) and 1.410(CN = 8) Å respectively).²⁷ The $\text{Sm}^{3+}\text{-O}$ distances (2.116(11)–2.364(10) Å) are in agreement with analogous ones in **1** (2.130(5)–2.408(3) Å). The intramolecular $\text{Sm}^{2+}\cdots\text{F}$ distances in **10** (2.697(9)–2.906(10) Å) are located within the range of published $\text{Sm}\cdots\text{F}$ interactions^{21,22} or slightly longer, however this does not lead to an appreciable elongation of C–F distances in CF_3 -groups.

The $\text{Y}^{3+}\text{-O}$ distances (2.115(3)–2.370(3) Å) are somewhat shorter than the lengths of the analogous $\text{Eu}^{3+}\text{-O}$ bonds in $\text{Eu}_3(\text{OR})_7(\text{DME})_2$ (2.160(4)–2.437(4) Å). The $\text{Y}\cdots\text{Eu}$ (3.6644(4), 3.6733(4) Å) distance is also somewhat smaller than the $\text{Eu}\cdots\text{Eu}$ distance (3.8602(3) Å) due to a smaller radius of Y^{3+} compared to the Eu^{2+} ion (1.040 (CN = 6) and 1.390 (CN = 8) Å respectively).²⁷ The $\text{Eu}^{2+}\text{-}\mu_2\text{-O}$ and $\text{Eu}^{2+}\text{-}\mu_3\text{-O}$ distances vary in the range of 2.473(3)–2.546(3) Å and 2.525(3)–2.811(3) Å respectively. These bond lengths in **11** are in agreement with analogous ones in $\text{Eu}_3(\text{OR})_7(\text{DME})_2$ ($\text{Eu}^{2+}\text{-}\mu_2\text{-O}$ 2.469(4)–2.532(3) Å and $\text{Eu}^{2+}\text{-}\mu_3\text{-O}$ 2.513(4)–2.740(4) Å). As with complex $\text{Eu}_3(\text{OR})_7(\text{DME})_2$ the intramolecular $\text{Eu}^{2+}\cdots\text{F}$ interactions are realized in complex **11**. The $\text{Eu}^{2+}\cdots\text{F}$ (2.662(2)–2.974(3) Å) distances are close to analogous ones in $\text{Eu}_3(\text{OR})_7(\text{DME})_2$ complex (2.699(4)–2.920(4) Å).



It is interesting to note that among the prepared alkoxides **1**, **3**, and **9–11** where intramolecular Ln...F interactions are observed, the steric saturation of the metal coordination sphere varies in the range of 87.7(2)–94.9(2)%. In turn, in complex **2** where such interactions are absent, the G-parameter (97.3 (2)%) significantly exceeds the analogous values for the complexes with close Ln–F contacts.

Luminescent properties

Among the prepared complexes, PL was observed for the europium–yttrium isopropoxide and all the cerium derivatives. Acetonitrile solutions of cerium compounds **4** and **6** showed emission in the region of 370–400 nm (Fig. 6). These bands exhibit multimodal character and each of them can be decomposed into two Gaussian peaks with maxima at 343, 373 and 392, 425 nm respectively. The energy difference between these peaks is close to 2000 cm^{-1} , in good agreement with the characteristic splitting of the two Ce^{3+} 4f ground levels induced by the spin–orbit interaction.²⁸ Therefore, the PL of **4** and **6** is attributed to the electric-dipole $4d \rightarrow 5f$ transitions in the cerium ion from the lowest excited state $^2D_{3/2}$ to the ground states $^2F_{5/2}$ and $^2F_{7/2}$.

Besides, the f–d emission of the Ce^{3+} ion was observed for complexes **3**, **8** and **9** (Fig. 7). Comparison of the PL spectra of **6** and **8** shows that insertion of the phenanthroline ligand in the cerium butanediolate caused slight blue shifting of the emission maximum from 410 to 405 nm and decreasing PL intensity.

Heterobimetallic complex **11** revealed blue PL with a maximum at 485 nm (Fig. 8). As the compound does not contain chromophore ligands and the band of emission lies in the range of Eu^{2+} luminescence,¹⁰ so the observed peak was attributed to $4f^6 5d^1 \rightarrow 4f^7$ transition in the europium(II) ion.

Interestingly, complexes **3** and **11** did not reveal luminescence in MeCN solution in contrast to THF medium probably

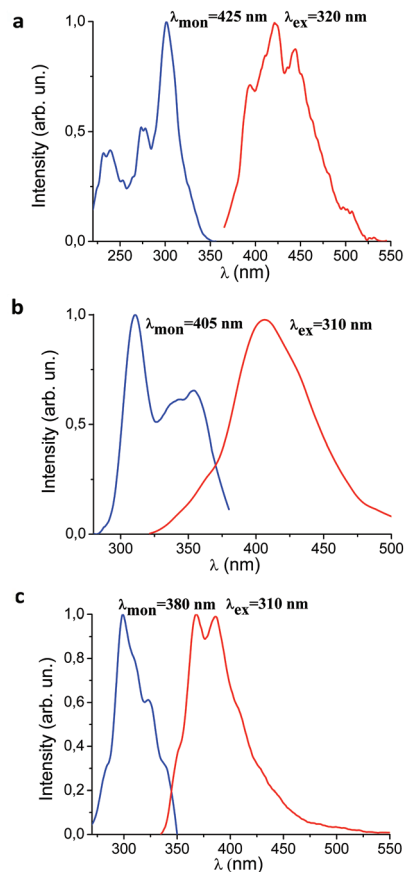


Fig. 7 Excitation (blue) and emission (red) spectra of complexes **3** (a) in THF, **8** (b) and **9** (c) in MeCN solution.

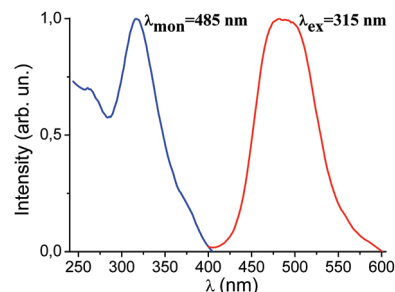


Fig. 8 Excitation (blue) and emission (red) spectra of THF solution of complex **11**.

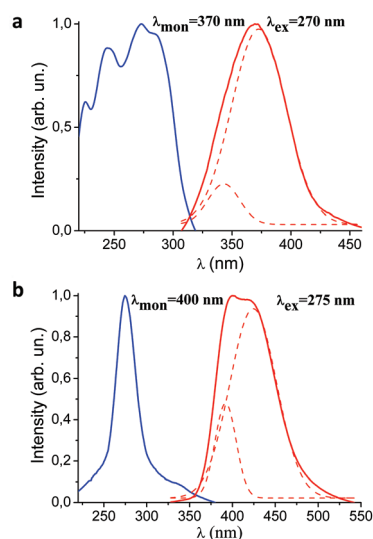


Fig. 6 Excitation (blue) and emission (red) spectra of complexes **4** (a) and **6** (b) in MeCN solutions, and Gaussian fits for the emission spectra of the alkoxides (red dashed lines).

because of differences in the symmetry of the crystal field at cerium atoms in these solvents.

As noted above, due to low volatility and thermal stability of the majority of the prepared complexes, the only OLED device based on isopropoxide **3** was fabricated. A simple three-layered device of structure ITO/TPD/complex **3**/BATH/Yb was prepared by the vacuum evaporation method. The diode displayed weak orange luminescence, the spectrum of which contained a single broad band with the maximum at 620 nm (Fig. 9). The EL efficiency did not exceed 2 cd m^{-2} at 30 V.



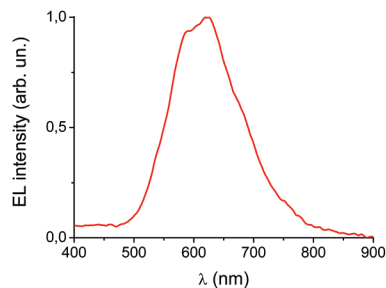


Fig. 9 EL spectrum of OLED of structure ITO/TPD/complex 3/BATH/Yb.

The observed EL can be ascribed to the emission of the electroplex formed at the TPD/3 interface. Confirmation of the supposition is the absence of PL of the double layer and blend TPD-3 samples. Similar EL of electroplex was registered previously for the OLED devices based on the lanthanide pentafluorophenolates.²⁹

Conclusions

A set of Ce(III), Sm(II/III), Eu(II), Gd(III) and Yb(III) complexes with fluorinated isopropoxide, *tert*-butoxide and butanediolate ligands was prepared. X-ray and LDI-TOF analysis revealed that Ln(III) isopropoxides as well as Ce *tert*-butoxide have binuclear arrangement whereas gadolinium butoxide is mononuclear probably due to a smaller radius of the Gd³⁺ ion. Isostructural alkoxides **10** and **11** are trinuclear clusters in which two Ln²⁺ cations are bonded *via* bridging RO ligands to the Sm³⁺ cation (in **10**) or the Y³⁺ cation (in **11**). All the prepared cerium complexes upon UV excitation showed short-wavelength emission at the region of 370–425 nm as broadened bands, which is characteristic for 5d→4f transitions in the cerium ion.³⁰ Heterobimetallic alkoxide **11** revealed blue PL with a maximum at 485 nm which was assigned to f–d emission of the europium(II) ion. Attempts to prepare OLED devices using the synthesized alkoxides as emitter layers for investigation of their EL properties failed because of low thermal stability of the compounds. The only complex, on the basis of which we were able to design a diode, was cerium compound **3** but this device displayed the electroplex luminescence and not the metal-centered emission.

Acknowledgements

This work was supported by the Russian Foundation for Basic Research (projects 13-03-00097, 14-03-31043, 15-33-20296).

Notes and references

- J. Kido and Y. Okamoto, *Chem. Rev.*, 2002, **102**, 2357–2368; J.-C. G. Bunzli and C. Piguet, *Chem. Soc. Rev.*, 2005, **34**,

- 1048–1077; M. A. Katkova, A. G. Vitukhnovskii and M. N. Bochkarev, *Russ. Chem. Rev. (Engl. Transl.)*, 2005, **74**, 1089–1109; G. F. de Sa, O. L. Malta, C. de Mello Donega, A. M. Simas, R. L. Longo, P. A. Santa-Cruz and E. F. da Silva Jr., *Coord. Chem. Rev.*, 2000, **196**, 165–195.
- 2 J. Shinar and R. Shinar, *J. Phys. D: Appl. Phys.*, 2008, **41**, 133001; S. Landgraf, *J. Biochem. Biophys. Methods*, 2004, **61**, 125–134; H. van Santen and J. H. M. Neijzen, *Jpn. J. Appl. Phys.*, 2003, **42**, 1110–1112.
- 3 C. Canevali, M. Mattoni, F. Morazzoni, R. Scotti, M. Casu, A. Musinu, R. Krsmanovic, S. Polizzi, A. Speghini and M. Bettinelli, *J. Am. Chem. Soc.*, 2005, **127**, 14681–14691; C. Tang, Y. Bando, D. Golberg and R. Ma, *Angew. Chem., Int. Ed.*, 2005, **44**, 576–579; L. Guerbous and O. Krachni, *J. Mod. Opt.*, 2006, **53**, 2043–2053.
- 4 P. Dorenbos, *J. Lumin.*, 2003, **104**, 239–260.
- 5 T. Yu, W. Su, W. Li, R. Hua, B. Chu and B. Li, *Solid-State Electron.*, 2007, **51**, 894–899.
- 6 W. Li, T. Mishima, G.-Y. Adachi and J. Shiokawa, *Inorg. Chim. Acta*, 1987, **130**, 277–281.
- 7 H. Kunkely and A. Vogler, *J. Photochem. Photobiol., A*, 2002, **151**, 45–47.
- 8 X.-L. Zheng, Y. Liu, M. Pan, X.-Q. Lu, J.-Y. Zhang, C.-Y. Zhao, Y.-X. Tong and C.-Y. Su, *Angew. Chem., Int. Ed.*, 2007, **46**, 7399–7403.
- 9 A. Strasser and A. Vogler, *Inorg. Chim. Acta*, 2004, **357**, 2345–2348.
- 10 J. Jiang, N. Higashiyama, K. Machida and G. Adachi, *Coord. Chem. Rev.*, 1998, **170**, 1–29.
- 11 C. P. Shipley, S. Capecchi, O. V. Salata, M. Etchells, P. J. Dobson and V. Christou, *Adv. Mater.*, 1999, **11**, 533–536.
- 12 D. M. Kuzyaev, R. V. Rumyantsev, G. K. Fukin and M. N. Bochkarev, *Russ. Chem. Bull. Int. Ed.*, 2014, **63**, 848–853.
- 13 P. B. Glover, A. P. Bassett, P. Nockemann, B. M. Kariuki, R. Van Deun and Z. Pikramenou, *Chem. – Eur. J.*, 2007, **13**, 6308–6320.
- 14 W. D. Buchanan and K. Ruhlandt-Senge, *Chem. – Eur. J.*, 2013, **19**, 10708–10715; W. D. Buchanan, M. A. Guino-o and K. Ruhlandt-Senge, *Inorg. Chem.*, 2010, **49**, 7144–7155.
- 15 P. Girard, J. L. Namy and H. B. Kagan, *J. Am. Chem. Soc.*, 1980, **102**, 2693–2698.
- 16 T. D. Tilley, R. A. Andersen and A. Zalkin, *Inorg. Chem.*, 1984, **23**, 2271–2276.
- 17 M. N. Bochkarev and A. V. Protchenko, *Equip. Exp. Tech.*, 1990, **1**, 194–195.
- 18 K. S. Mazdiyasi and B. J. Schaper, *J. Less-Common Met.*, 1973, **30**, 105–112; D. C. Bradley, H. Chudzynska, M. E. Hammond, M. B. Hursthouse, M. Motevalli and W. Ruowen, *Polyhedron*, 1992, **11**, 375–379.
- 19 K. K. Yan, G. Schoendorff, B. M. Upton, A. Ellern, T. L. Windus and A. D. Sadow, *Organometallics*, 2013, **32**, 1300–1316.
- 20 B. Liu, T. Roisnel, L. Maron, J.-F. Carpentier and Y. Sarazin, *Chem. – Eur. J.*, 2013, **19**, 3986–3994.
- 21 W. J. Evans, K. J. Forrestal, M. A. Ansari and J. W. Ziller, *J. Am. Chem. Soc.*, 1998, **120**, 2180–2181.



- 22 S. Bannerjee, T. J. Emge and J. G. Brennan, *Inorg. Chem.*, 2004, **43**, 6307–6312.
- 23 A. Guzei and M. Wendt, *J. Chem. Soc., Dalton Trans.*, 2006, 3991–3999.
- 24 H. Yin, J. R. Robinson, P. J. Carroll, P. J. Walsh and E. J. Schelter, *Chem. Commun.*, 2014, **50**, 3470–3472.
- 25 D. Werner, G. B. Deacon, P. C. Junk and R. Anwander, *Chem. – Eur. J.*, 2014, **20**, 4426–4438.
- 26 C. Janiak, *J. Chem. Soc., Dalton Trans.*, 2000, 3885–3896.
- 27 R. D. Shannon, *Acta Crystallogr., Sect. A: Cryst. Phys., Diffraction, Theor. Gen. Cryst.*, 1976, **32**, 751–767.
- 28 S. T. Frey and W. DeW. Horrocks Jr., *Inorg. Chem.*, 1991, **30**, 1073–1079.
- 29 A. P. Pushkarev, V. A. Ilichev, A. A. Maleev, A. A. Fagin, A. N. Konev, A. F. Shestakov, R. V. Romyantzev, G. K. Fukin and M. N. Bochkarev, *J. Mater. Chem. C*, 2014, **2**, 1532–1538.
- 30 A. Vogler and H. Kunkely, *Inorg. Chim. Acta*, 2006, **359**, 4130–4138.

